Automotive and Engine Technology (2025) 10:16
https://doi.org/10.1007/s41104-025-00163-9

ORIGINAL PAPER

An experimental and computational analysis of backfire initiation and propagation in a single-cylinder hydrogen port-fuel-injection engine

Brijesh Kinkhabwala[1] · Koushal Krishna[1] · Florian Reppert[1] · Uwe Wagner[1] · Thomas Koch[1]

Received: 17 November 2025 / Accepted: 27 November 2025

Abstract
The global push for defossilization necessitates the advancement of hydrogen internal combustion engines as a key solution for the heavy-duty transport sector. However, the distinct combustion properties of hydrogen, particularly its high reactivity, introduce operational challenges for port-fuel-injected (PFI) engines, most critically the risk of backfire—the uncontrolled ignition in the intake system. This phenomenon not only makes the engine potentially unsafe for operation but also severely limits the achievable power density and combustion stability. Addressing this barrier requires a comprehensive understanding of the complex interactions between various engine control parameters. This study presents a coordinated experimental and computational fluid dynamics (CFD) investigation focusing on strategies to mitigate backfire in a single-cylinder, heavy-duty hydrogen PFI engine. The influence of engine parameters such as injector location, start of injection (SOI) timing, backpressure, engine valve timing and injection pressure and duration on mixture formation, and backfire onset were also analyzed. The findings establish critical guidelines for defining the stable operating window, demonstrating how the tuning of key control variables can effectively promote mixture preparation, reduce backfire instances and potentially increase engine efficiency. This research provides an essential framework for the reliable, safe and efficient deployment of hydrogen PFI technology in future low-carbon transportation applications.

Keywords Hydrogen ICE · Port fuel injection · Backfire · Experiment · Simulation · Valve timing · Back pressure

1 Introduction

The transportation sector remains one of the largest contributors to global greenhouse-gas emissions, with more than 90% of its energy demand still met by gasoline and diesel combustion [1]. Road transport alone accounts for approximately 7.5 Gt of CO_2 emissions annually, making defossilization or decarbonization of this sector a crucial step toward global climate targets [2]. Hydrogen has emerged as a viable regeneratively produced, defossilized alternative fuel for internal combustion engines (ICEs) and fuel-cell applications due to its high energy content per unit mass (120 MJ/kg), wide flammability limits (4–75%), and clean combustion characteristics [3]. When derived from renewable sources, hydrogen combustion eliminates CO_2 emissions at the tailpipe, with only trace CO_2 generated from lubricating-oil oxidation [4]. Demonstration studies on heavy-duty H_2-ICEs have already reported tailpipe CO_2 reductions exceeding 99% compared to diesel baselines, achieving values as low as 0.4 g/kWh CO_2 under regulatory cycles [5]. Simultaneously, engine efficiencies exceeding 40% have been achieved under lean operation [6].

However, hydrogen's distinct combustion properties—low ignition energy (0.02 mJ), high diffusivity, and a laminar flame speed up to seven times that of gasoline—pose significant control challenges for stable operation in premixed conditions [7]. In particular, the elevated adiabatic flame temperature of hydrogen–air mixtures promote

✉ Brijesh Kinkhabwala
brijesh.kinkhabwala@kit.edu

Koushal Krishna
uxghr@student.kit.edu

Florian Reppert
florian.reppert@kit.edu

Uwe Wagner
uwe.wagner@kit.edu

Thomas Koch
thomas.a.koch@kit.edu

[1] Institute of Internal Combustion Engines (IFKM), Karlsruhe Institute of Technology (KIT), Karlsruhe, Germany

Published online: 09 December 2025

thermal NO_X formation through the extended Zel'dovich mechanism, which becomes dominant at temperatures above approximately 1800 K [8]. Consequently, mitigation strategies such as exhaust gas recirculation (EGR) and water injection have been employed to suppress NO_X by reducing in-cylinder temperature and oxygen concentration [9]. For instance, cooled EGR at 25% volume fraction has been shown to cut NO_X emissions by up to 57%, while water injection with a water-to-hydrogen ratio (WHR) of 7.5 reduced NO_X by approximately 97% without introducing combustion instability [10].

A major operational barrier for port-fuel-injected (PFI) hydrogen engines is backfire—the unintended ignition of the fresh charge within the intake port or manifold prior to intake-valve closure [11]. Backfire not only damages intake components but also constrains the feasible range of spark timing, mixture preparation, and fuel injection scheduling [12]. The phenomenon arises primarily due to residual hot gases or wall hot spots near the intake valve, flame propagation during valve overlap, or excessive fuel–air mixture concentration in the intake manifold [13]. Pressure sensors in the intake manifold have demonstrated that backfire events can be identified by pressure-wave signatures propagating upstream, allowing precise localization and intensity estimation of such events [14]. High-speed optical techniques in single-cylinder hydrogen engines have further revealed that manifold ignition frequently originates near exhaust-valve edges during the overlap phase, where residual gases act as ignition sources [15].

Mitigation approaches to date have focused on injection phasing, injector geometry, and intake-valve timing adjustments [16]. Lu et al. (2024) demonstrated that controlling start of injection (SOI) within − 430 to −360°CA ATDC effectively reduced backfire probability by nearly eliminating hydrogen presence during valve overlap [12]. Similarly, increased injection pressure enhances fuel jet penetration and mixing uniformity, reducing localized hydrogen concentration and backfire risk [17]. Injector configuration studies have found that transitioning from a single to a dual-injector system can increase maximum brake power output by 42.3% due to improved mixture preparation and reduced unburned hydrogen in the port [18].

The present study aims to address this gap through a comprehensive parametric investigation of factors influencing backfire in a port-fuel-injected hydrogen engine. Specifically, it examines how coordinated variations in SOI, injector sleeve geometry, injection pressure, and duration, together with intake back pressure and valve phasing, affect backfire onset and frequency. By systematically mapping these parameters, the study seeks to delineate operating regions that minimize backfire while maintaining engine performance, contributing to the safe and efficient implementation of hydrogen PFI engines within future low-carbon transport systems.

1.1 Experimental setup

The experimental investigations were carried out on a single-cylinder, four-stroke, spark-ignition base CNG engine representative of heavy-duty truck applications. The engine had a compression ratio of 13.4:1 and a total displacement of 1283 cm³, equipped with a flat-roof cylinder head and a four-valve configuration (two intake and two exhaust valves) to enhance volumetric efficiency. A schematic representation of the experimental setup is provided in Fig. 1, illustrating the overall engine architecture and key components integrated into the test facility. The engine was mounted on a steady-state dynamometer within a fully instrumented test cell equipped with state-of-the-art measurement and control systems. The test facility was capable of capturing high-frequency engine operating parameters, which were recorded and processed using the AVL INDIMASTER ADVANCED data acquisition system. In-cylinder pressure measurements were obtained using a Kistler piezoelectric pressure

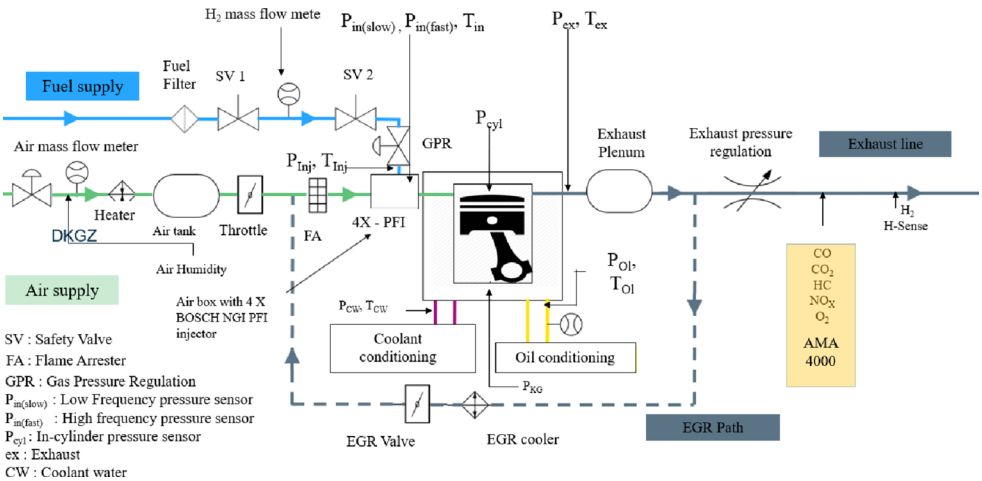

Fig. 1 Schematic of the single-cylinder heavy-duty H_2-ICE experimental test cell setup

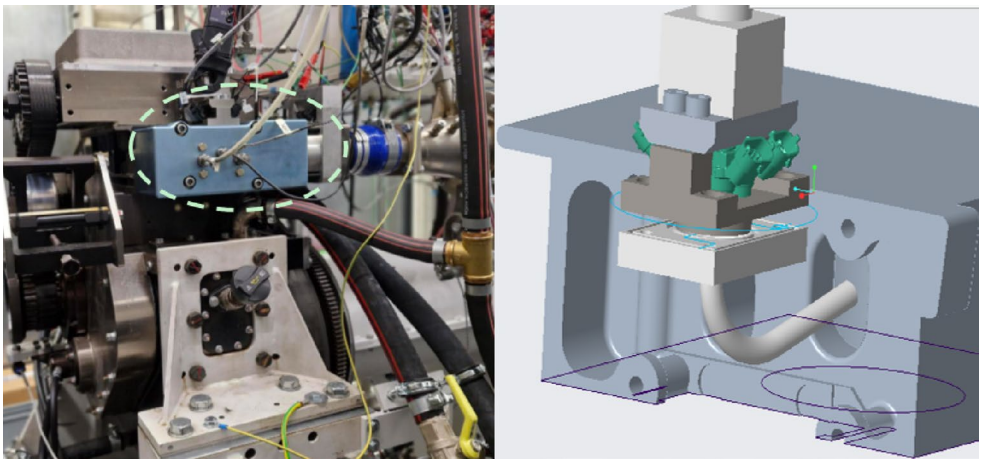

Fig. 2 Experimental test rig setup and Port-Fuel Injection (PFI) module design

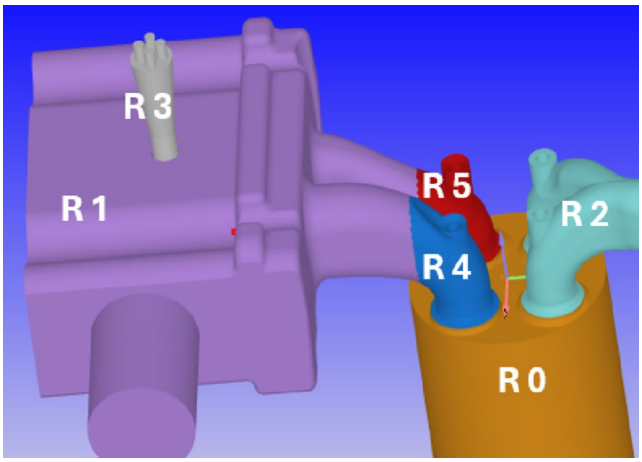

Fig. 3 Computational domain and region definition for 3D CFD simulation. R0 - combustion chamber, R1 - intake chamber, R2 - exhaust ports, R3 - H2 injector and sleeve, R4 and R5 - intake ports

transducer mounted on the cylinder head. Additional high-frequency pressure sensors were installed on both the intake and exhaust manifolds to enable detailed data acquisition for combustion analysis, computational fluid dynamics (CFD) model validation, and backfire detection. The acquired pressure data were also utilized to activate safety mechanisms in real time during hydrogen engine operation. Both low- and high-frequency pressure sensors were employed to monitor transient pressure fluctuations and identify backfire events. Flame arresters were installed upstream of the pressure sensors to suppress any back-propagating hydrogen flames in the intake system. The test cell was integrated with a closed-loop safety control system operated through MORPHEE software, allowing automated actuation of safety valves in the event of a detected backfire. Exhaust gas emissions were quantified using an EMA 4000 ADVANCED emission measurement system, which included, a CLD 4000 analyzer for NO_x measurement (0–1000 ppm), an FID 4000 analyzer for total hydrocarbon (THC) measurement (0–2000 ppm), and an IRD 4000 (FR) analyzer for CO measurement (0–500 ppm). In the preliminary stage, the base CNG engine was retrofitted with a BOSCH NGI injector and operated under various test conditions to evaluate injector performance, back-pressure effects, and overall combustion stability. Based on these trials, medium- and high-load conditions were selected for a detailed investigation of backfire phenomena. The operating points corresponding to 10 bar and 15 bar indicated mean effective pressure (IMEP) at 1100 rpm were analyzed comprehensively. The hydrogen conversion process was achieved with minimal modifications to the baseline CNG engine configuration, ensuring the preservation of its fundamental design and operational integrity.

The above images show the engine installed on a steady-state dynamometer test cell, with the marked circle indicating the port fuel injection (PFI) module. A simplified schematic of the PFI module is shown on the right side of Fig. 2. The CAD model of the intake manifold is equipped with four Bosch NGI injectors (each with a maximum flow rate of 2.5 kg/s), arranged in a 2×2 configuration on opposite sides of the module. Each pair of injectors feeds into a common injector sleeve with an angled elbow (section view presented in Fig. 4), which directs the hydrogen toward the larger intake port (R4 in Fig. 3) to ensure optimal fuel delivery. This design was finalized after multiple CFD-based iterative studies to optimize fuel spray distribution. Detailed discussion on the injector location optimization is provided in a subsequent section.

1.2 CFD simulation setup

3D CFD simulations in this study were performed using the commercial solver CONVERGE v4.1, applying a Reynolds-Averaged Navier-Stokes (RANS) framework. The refinement criteria were based on velocity, temperature, and hydrogen species mass fraction, with respective threshold values of 0.1 m/s, 2.5 K, and 1×10^{-4}. Special attention was given to fuel species-based AMR, critical in hydrogen-fueled

engines due to hydrogen's high diffusivity—often overlooked in hydrocarbon-based engines but essential here for accurate jet resolution. A variable time-step algorithm was implemented, using a minimum time step of 1×10^{-10} s, and CFL limits of 1 (convection), 2.0 (diffusion), and 50.0 (Mach). A detailed grid sensitivity analysis was conducted to optimize accuracy and computational cost. The final grid configuration included a base grid size of 3,6 mm, injector region embedding down to 0.225, and AMR refinement to 0.45 mm in critical zones, further refined to 0.225 mm near boundaries.

The entire CFD domain was divided into several individual regions following standard CFD modeling practices. To accurately capture the species concentration at critical locations—such as the intake valve, intake port, intake manifold, and within the hydrogen injector sleeve—the computational domain was further subdivided into specific regions, as illustrated in the CFD model shown in Fig. 3. The regions were defined as follows: Region 0 – Cylinder, Region 1, 4, and 5 – Intake system, Region 2 – Exhaust system, and Region 3 – Hydrogen injector and sleeve.

2 Results and discussion

2.1 Injector location variation

The quantity of residual hydrogen is a critical factor in hydrogen-fueled engines, as excessive residual hydrogen in the intake can increase the risk of backfire and reduce engine power output by displacing fresh charge. It also contributes to higher cycle-to-cycle variations, thereby compromising engine stability and performance. Therefore, the influence of injector positioning on the residual hydrogen concentration within the intake chamber was investigated utilizing three different injector configurations. In version 1 (Fig. 4a), the injector was positioned at the midpoint between the two intake ports. This placement was intended to evenly distribute the injected hydrogen between the ports, theoretically enhancing mixture uniformity. In contrast, versions 2 and 3 (Fig. 4b and c) placed the injector within regions 5 and 4, respectively. These locations were chosen to minimize interference with the intake airflow, thereby reducing the likelihood of backflow and promoting smoother hydrogen delivery. However, the simulation results (Fig. 5(a) and (b)) reveal that these initial assumptions were only partially valid. While Version 1 was expected to improve homogeneity, it introduced physical obstructions to the incoming hydrogen stream, leading to a higher residual hydrogen mass within the intake chamber. This increased residual content not only degraded mixture uniformity but also increased the risk of backfire. Conversely, Versions 2 and 3 showed significantly lower residual hydrogen masses after the completion of injection. The difference between these two configurations was negligible, indicating that both provided similar performance benefits by reducing flow obstruction and mitigating hydrogen accumulation in the intake.

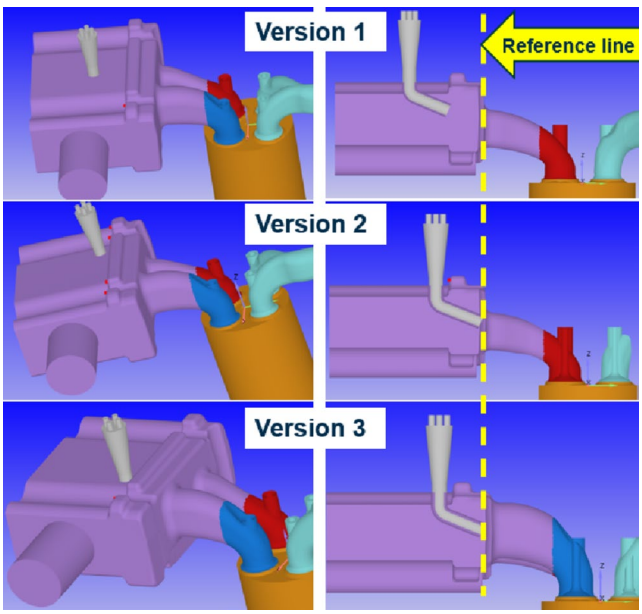

Fig. 4 Top: version 1 – PFI injector positioned along the center line between the larger and smaller intake ports. Middle: version 2 – PFI injector located near the smaller intake port. Bottom: version 3 – PFI injector located near the larger intake port

To exclude any discrepancies in flow due to the physical obstruction of the injector when its location is changed, a separate simulation was carried out comparing the mass flow rate and the crank angle for all three versions. From the results in Fig. 6(a) and (b), it is found that before SOI and after EOI, the mass flow remains the same in both ports and changes in flow are only observed after injection begins. Hence, it can be concluded that the differences observed in residual mass of hydrogen in the different versions is solely due to changing flow characteristics caused by the variation of the injector location and not a result of the injector's geometry.

2.2 Influence of SOI timing variation

This subsection investigates the effects of start of injection (SOI) timing variation on in-cylinder charge mixing and fuel delivery to establish guidelines for improving engine efficiency and mitigating adverse phenomena such as backfire. Six SOI timings, spaced at 20° intervals between 340°CA and 440°CA, were simulated to identify trends in mixture homogeneity (for efficiency optimization) and residual hydrogen mass in the intake and combustion chambers (for backfire prevention). From the results illustrated in Fig. 7, both excessively advanced and retarded SOI timings were

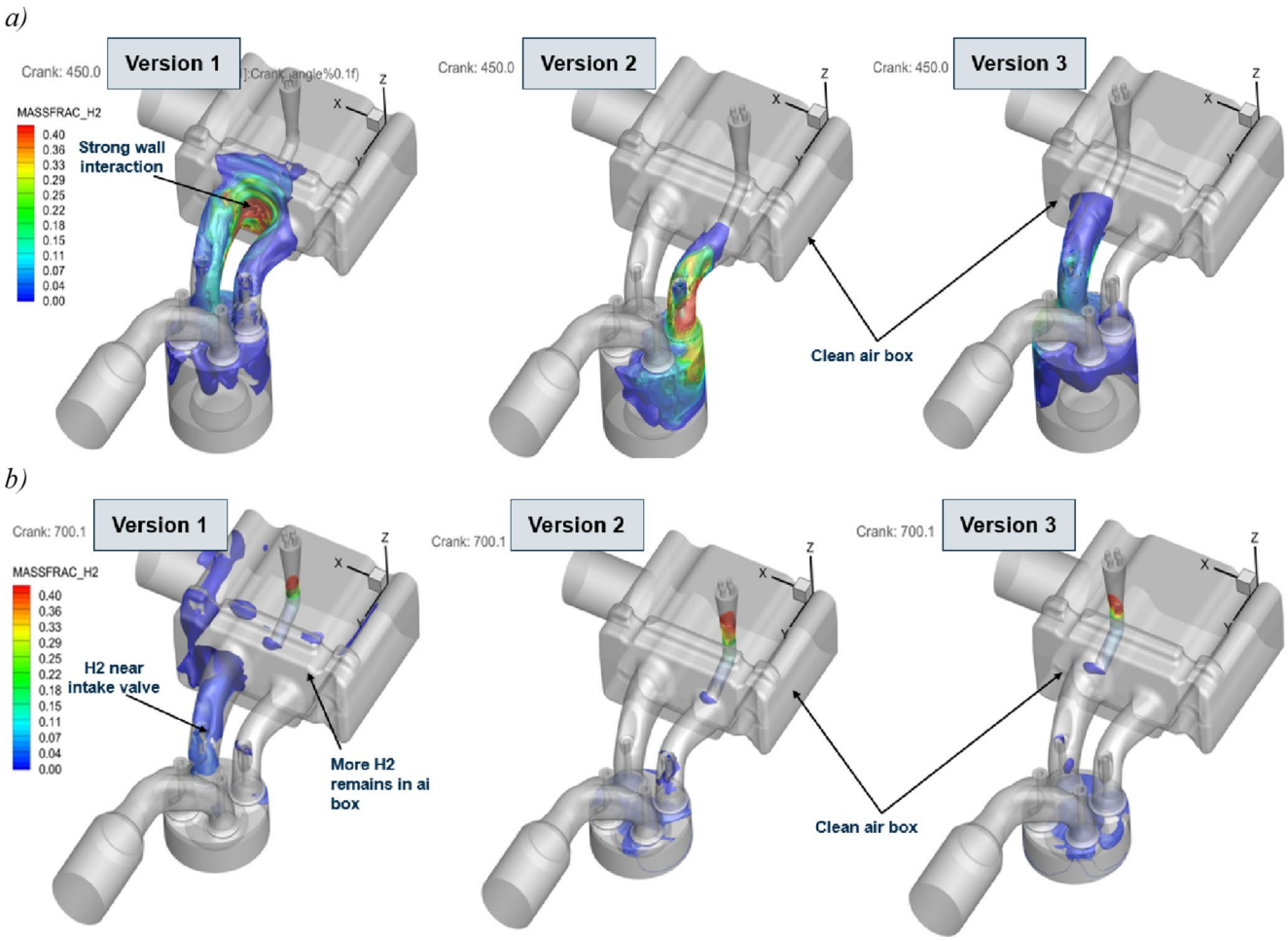

Fig. 5 Effect of injector location on hydrogen mass fraction and residual accumulation at (**a**) 450°CA, and (**b**) 700°CA

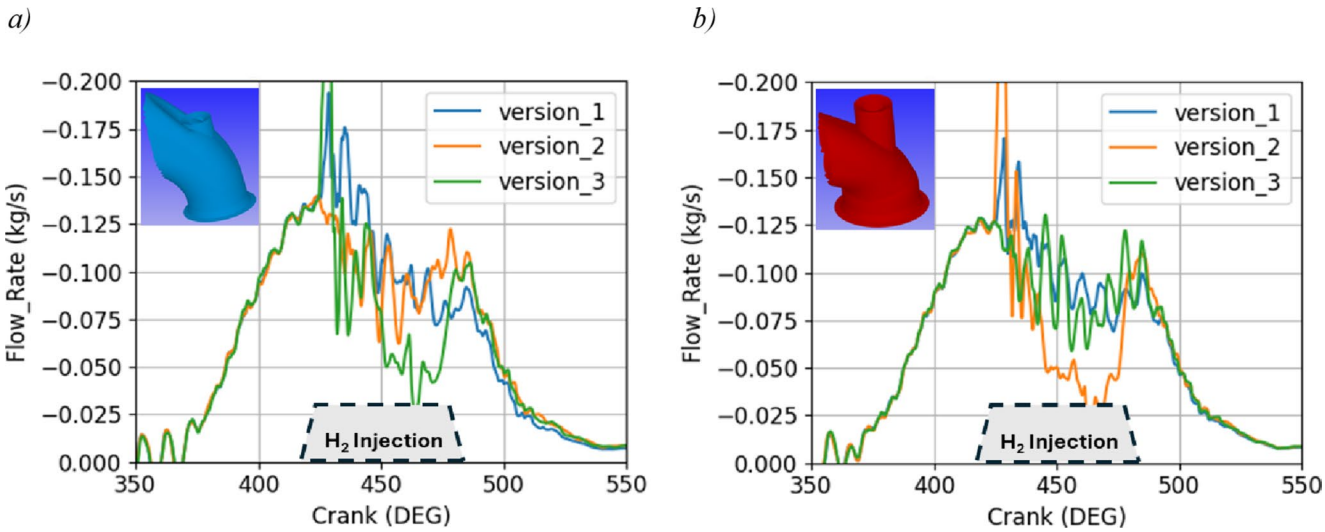

Fig. 6 Comparison of mass flow rate the three injector configurations, Fig. 6 (**a**) Region 5, and (**b**) Region 4.

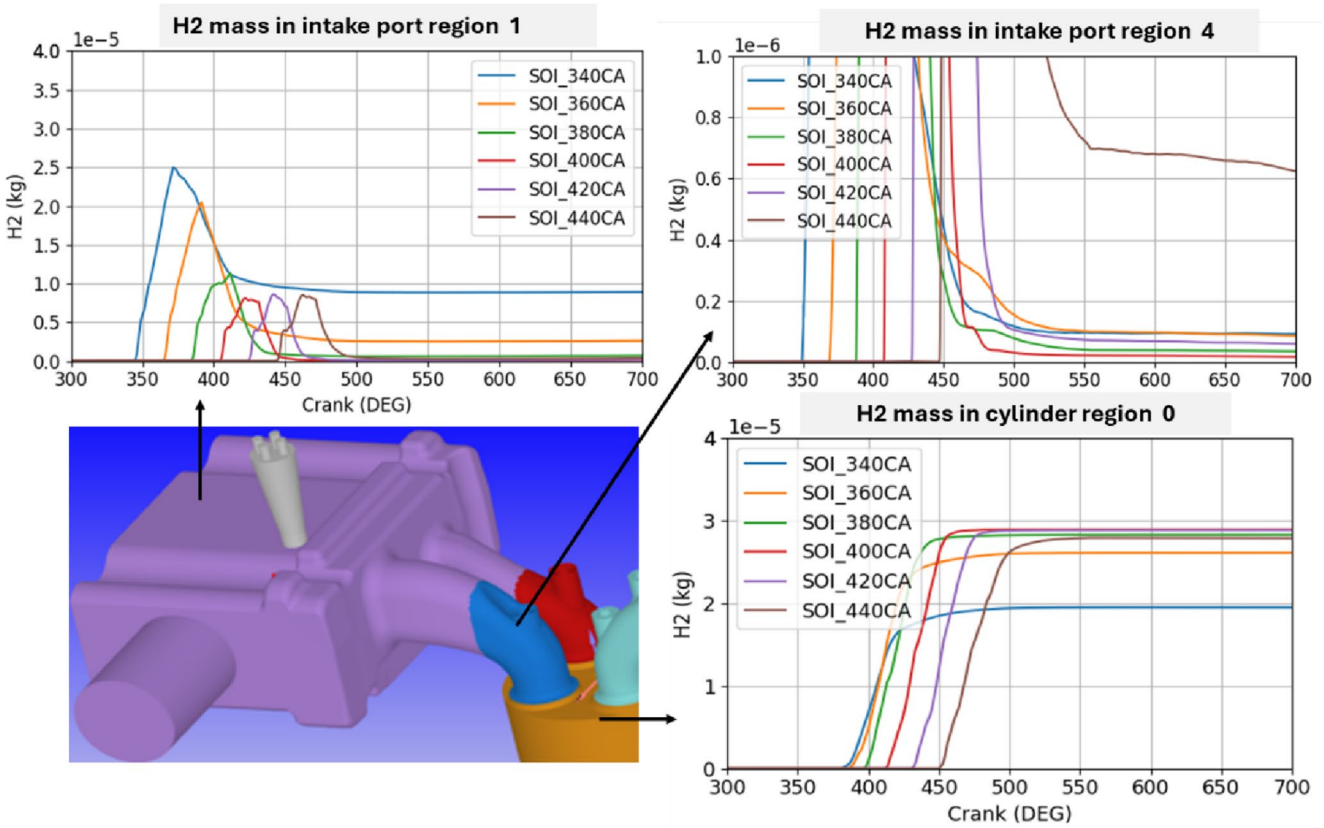

Fig. 7 Hydrogen mass in key computational regions as a function of start of injection (SOI) timing

found to increase hydrogen retention in undesired regions of the intake system. When the SOI is too early, the intake valve is not yet sufficiently open to allow complete hydrogen entry into the cylinder, leading to partial fuel entrapment within the intake port and consequently elevating the risk of backfire. Conversely, very late SOI timings result in incomplete cylinder filling, where a portion of hydrogen remains unadmitted, contributing to incomplete combustion and elevated residual hydrogen levels. The key distinction between these cases lies in the location of unburned hydrogen accumulation: early SOI promotes hydrogen build-up in the intake manifold or plenum, while late SOI causes hydrogen to concentrate near the intake valve—closer to potential ignition sources and thus posing a higher backfire risk. The variation of SOI timing also strongly influences mixture homogeneity. Theoretically, an early SOI provides more time for thorough mixing of hydrogen with intake air, yielding the highest homogeneity. In contrast, late SOI restricts the available mixing time, leading to poorer mixture uniformity. Mid-range SOI timings at 20 to 30% of intake valve lift, offer a favorable compromise between these two extremes. During this period—typically the mid-phase of the intake stroke—the intake air entering through the ports establishes a strong in-cylinder flow field that guides the subsequent hydrogen injection. The injected hydrogen follows this flow, forming a “sandwich-like” mixture consisting of an air layer, an air–hydrogen blend, and a subsequent air layer. This structure enhances the distribution of hydrogen and improves mixture uniformity compared to late injection, though it remains slightly less homogeneous than the early SOI case due to reduced mixing duration. Apart from this, the in-cylinder fuel mass also varies with different SOI timings, as shown by the H_2 mass in the cylinder region (Fig. 7), which in turn affects the engine’s cyclic performance. The Simulation results presented in Fig. 8(a) and (b) confirm these trends: early injection results in the most uniform mixture but can increase residual hydrogen in the intake, while late injection yields the highest residual mass and the least homogeneity.

A moderate SOI window, approximately between 380°CA and 400°CA (approximately 20–30% of valve lift) for an injection duration of 60°CA, therefore represents an optimal compromise. This range ensures adequate hydrogen delivery into the cylinder while balancing the competing objectives of achieving mixture uniformity and minimizing backfire risk.

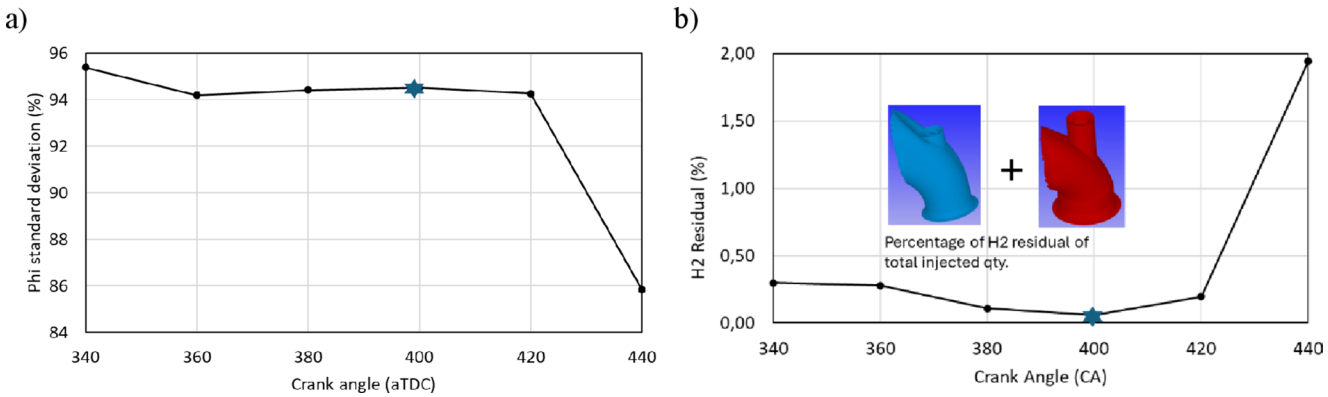

Fig. 8 Impact of back pressure on exhaust gas backflow and intake temperature

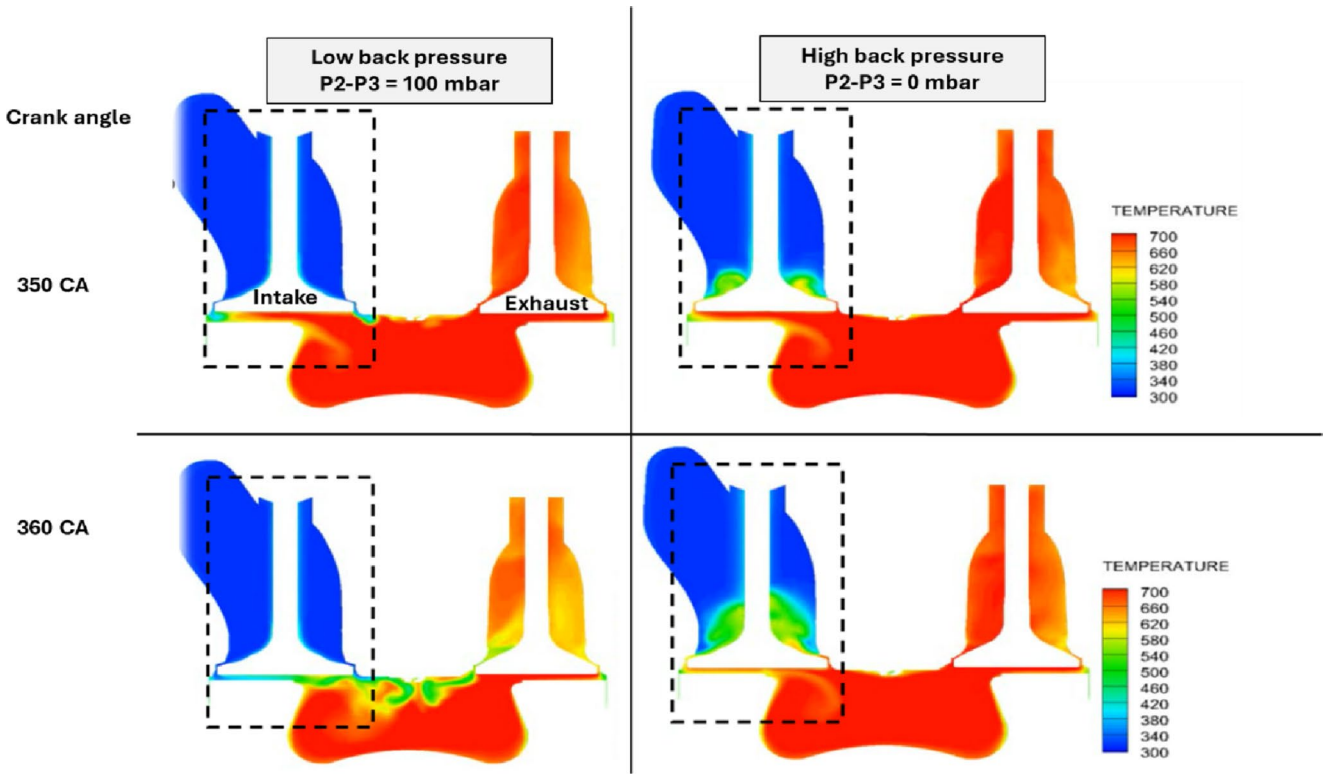

Fig. 9 Engine operation logs at high back pressure (P2 = P3)

2.3 Influence of back pressure variation

To replicate the pressure conditions induced by a turbocharger in a real engine and to ensure proper exhaust gas recirculation (EGR) drivability, back pressure regulator valves were installed along the exhaust pipe to control the desired exhaust pressure. Theoretically, an increase in back pressure enhances the tendency for exhaust gas backflow, as the exhaust products must overcome a higher pressure gradient during the exhaust stroke. This theoretical effect is directly supported by the simulation results in Fig. 9. Comparing the high back pressure case (P2-P3 = 0 mbar) to the low back pressure case (P2-P3 = 100 mbar) at 360°CA, the high back pressure condition clearly shows a larger, hotter plume of exhaust gas concentrated near the intake valve. This visual evidence confirms that the expulsion of exhaust gases becomes incomplete, resulting in a fraction of hot residual gases remaining trapped within the cylinder—commonly referred to as internal EGR.

The presence of these hot residuals elevates the in-cylinder temperature and, consequently, increases the likelihood of backfire due to auto-ignition. Moreover, this higher back pressure exerts an opposing force against the intake airflow during the valve overlap phase, further promoting reverse

flow and mixture instability. The engine logs (Fig. 10) for operation at base valve timing show distinct backfire events: a consequence of the effects discussed earlier that are produced by high back pressure. These events are characterized by rapid fluctuations in intake pressure and temperature, as captured by the respective sensors. At low-load operation (engine torque≈60 Nm), the occurrence of backfire is less frequent, though still observable through sharp intake temperature peaks. As the engine load increases to approximately 80 Nm, backfire events become more pronounced due to the intensified back pressure effect. Backfire, knocking, and misfire are generally sequential phenomena; when the engine experiences sudden load transitions, the lubricating oil film between the piston ring and liner may momentarily breach into the combustion chamber. The entrained oil subsequently burns in the following combustion cycles, contributing to elevated total hydrocarbon (THC) and carbon monoxide (CO) emissions. The correlation between backfire occurrences, intake temperature spikes, and the simultaneous rise in HC and CO emissions strongly supports this interpretation.

2.4 Valve timing variation

2.4.1 Valve timing variation under moderate back pressure

Four valve timing configurations (illustrated in Fig. 11) were examined: base valve timing (control), early exhaust valve opening, late intake valve opening, and no overlap (combining early exhaust and late intake valve opening). Injection timing and duration were kept constant (420–460°CA) for all cases. Simulation results presented in Fig. 12 indicate that the late intake valve opening configuration exhibits the lowest risk of backfire, as both backflow velocity and flow rate are minimal. This behavior can be attributed to the fact that in the base and early exhaust valve timing cases, in-cylinder pressure remains high as the piston is still moving upward as the intake valve opens. This therefore increases the risk of backfire.

In the no-overlap configuration, the elevated in-cylinder pressure that contributes to backflow in other cases does not occur. However, the absence of valve overlap eliminates the scavenging effect—i.e., the flushing of residual gases out through the exhaust port by the incoming air entering from the intake side. With the exhaust valve fully closed during intake valve opening, hot exhaust products tend to remain

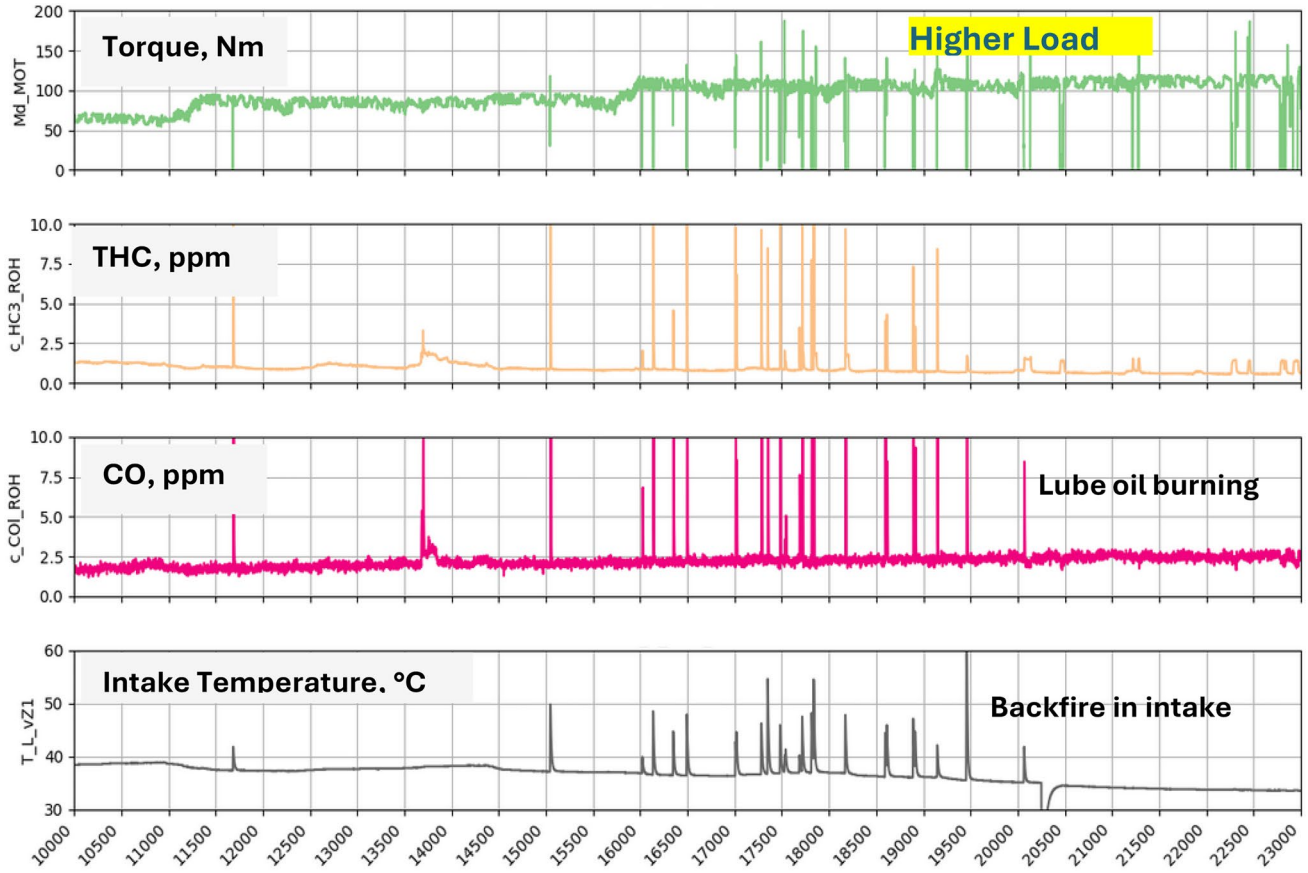

Fig. 10 Engine operation logs at high back pressure (P2=P3)

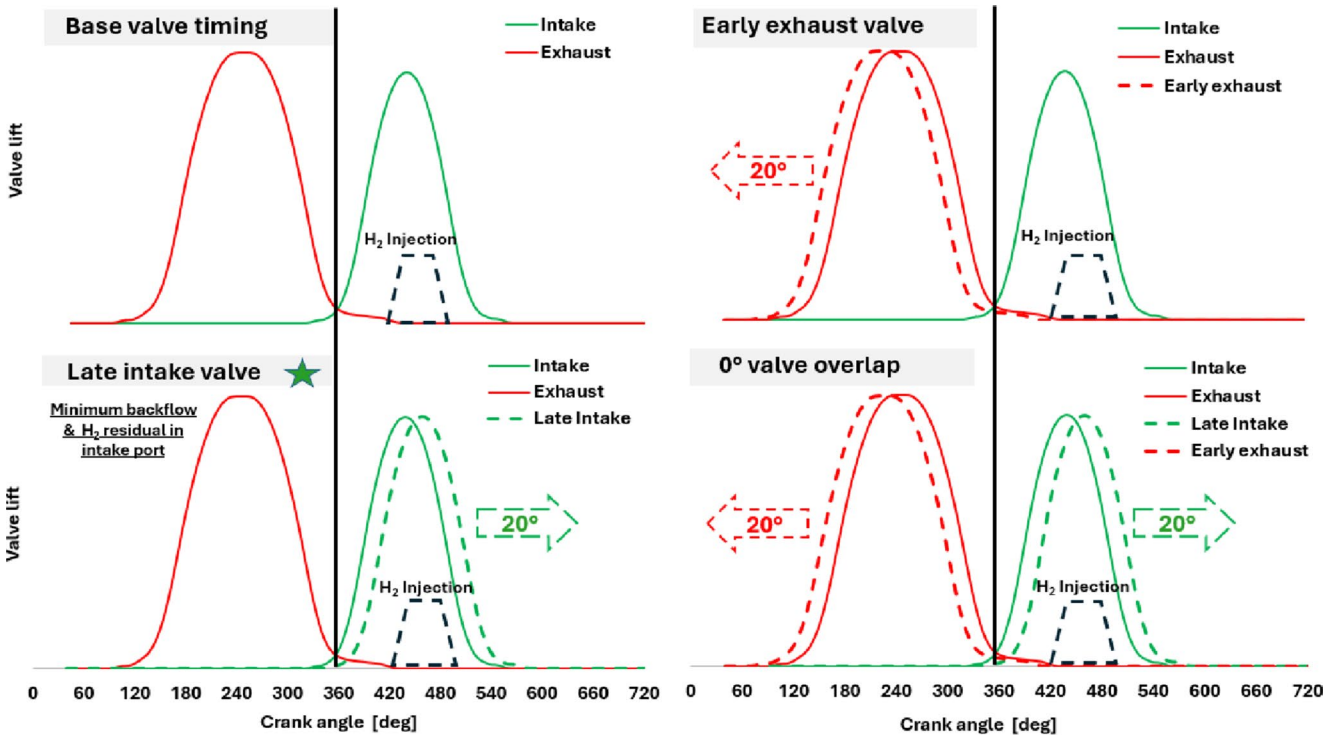

Fig. 11 Investigated valve timing configurations at fixed PFI injection window

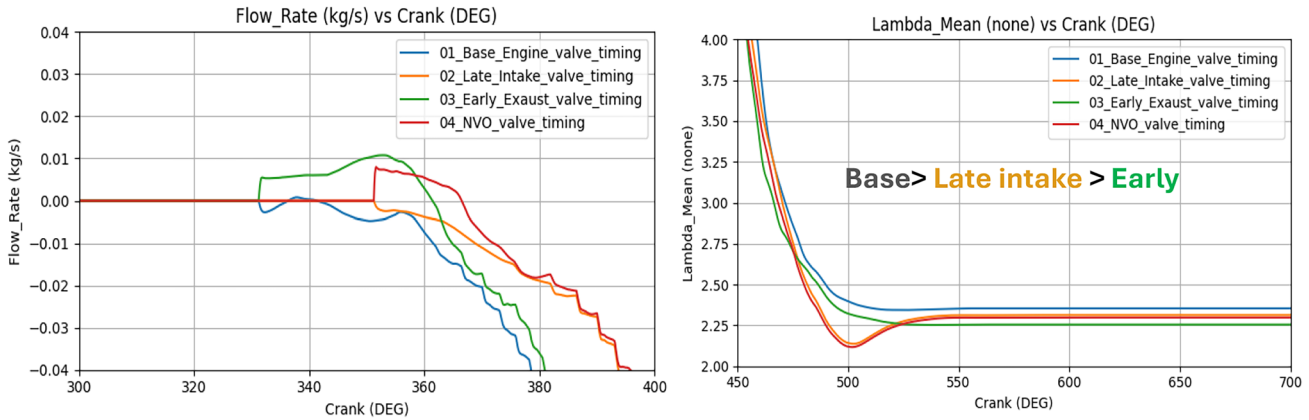

Fig. 12 Comparison of backflow and thermodynamic parameters for different valve timings

near the intake valve, increasing the likelihood of auto-ignition and subsequent backfire. As with SOI variation, modifying the intake and exhaust valve timing influences both backfire tendency and mixture homogeneity. From Fig. 12, it is observed that the base valve timing promotes slightly higher mixture uniformity compared to the early exhaust and late intake cases; however, the difference in homogeneity is not substantial. Consequently, the late intake valve timing is identified as the optimal configuration, as it significantly reduces backfire risk without materially compromising mixture uniformity.

2.4.2 Valve timing optimization under high back pressure

Valve timing was varied between the base valve and late intake valve timing in an engine running at 1200 rpm under conditions where the back pressure was maintained equal to the intake pressure ($P_2 = P_3$), representing a relatively high-pressure scenario. Although the late intake valve timing is expected to exhibit reduced backfire incidence for reasons discussed in Sect. 2.4.1, additional simulations were performed to visualize its effects under realistic engine conditions. Figure 13 presents the temperature distribution across intake, exhaust, and combustion chambers. As the cycle progresses from 350°CA to 360°CA, the intake port

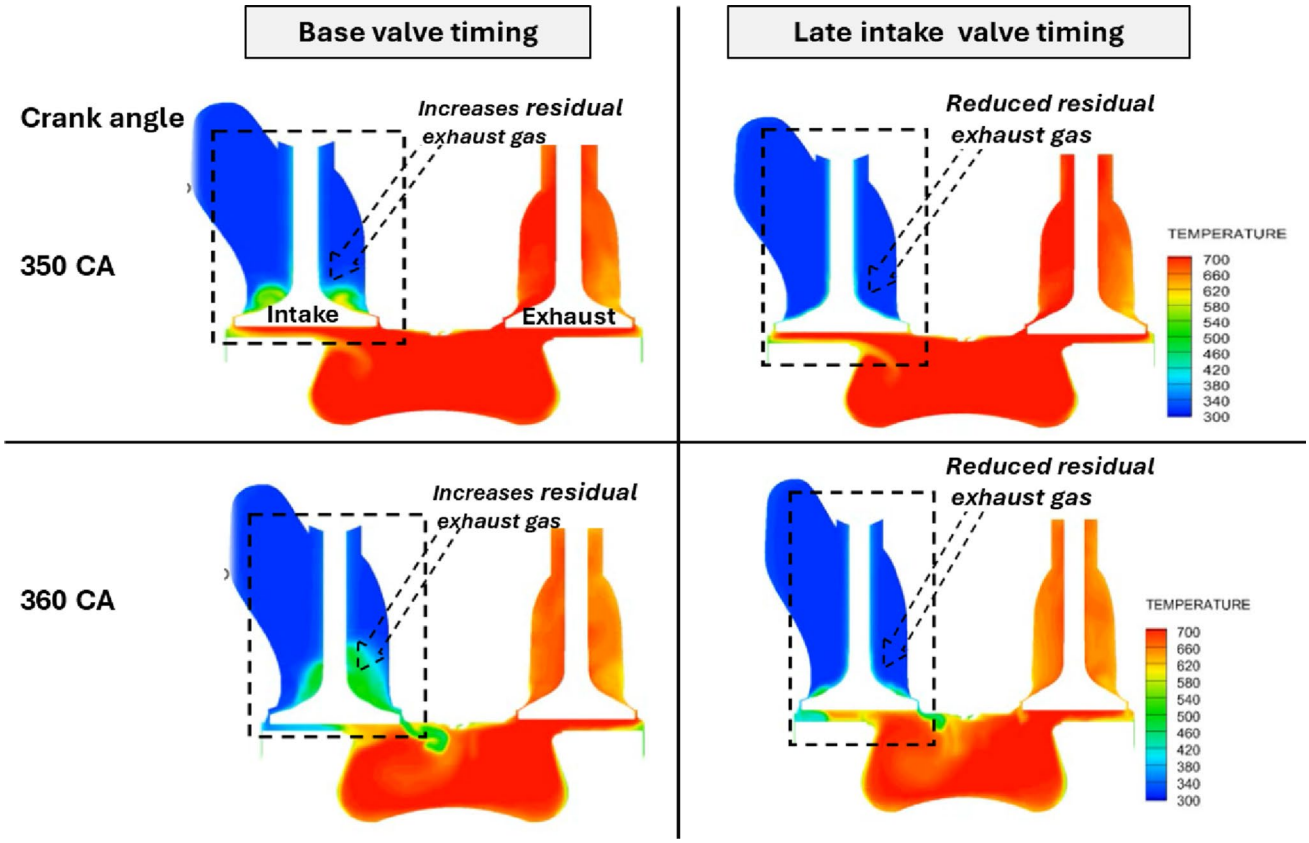

Fig. 13 Temperature distribution during valve overlap under high back pressure

temperature in the base valve timing case rises significantly compared to that in the late intake valve case. This temperature increase arises from the backflow of hot exhaust gases into the intake port, driven by elevated in-cylinder pressure as previously described. Accordingly, even for higher-load engine operation—particularly under exhaust gas recirculation (EGR) or turbocharged conditions—the late intake valve timing configuration represents the optimal choice, effectively minimizing backfire potential while maintaining stable combustion behavior.

2.4.3 Optimized SOI for the late intake valve timing case

This subsection extends the analysis using the same experimental and simulation parameters described previously, now incorporating the optimized SOI timing identified in Sect. 2.2 in combination with the late intake valve timing configuration. This combined approach aims to further reduce hydrogen residual accumulation and mitigate backfire under both moderate and high back-pressure conditions.

Figure 14 presents the temperature distribution and residual hydrogen mass fraction across intake, exhaust, and combustion chambers. Furthermore, experimental results, represented as engine operation logs, are plotted in Fig. 15. All simulation and experimental parameters were maintained consistent with those used in Sect. 2.3 to ensure comparability and reliability of results. The optimal Start of Injection (SOI) was determined to be 400°CA for the base valve timing configuration and 380°CA for the late intake valve timing configuration, based on the analysis methods already discussed in Sect. 2.2.

As shown in Fig. 14, when the base and late intake valve timing configurations are compared to each other at their respective optimal SOI timings, a noticeable reduction in residual hydrogen mass is observed near the intake valve and within the intake port in the late intake valve timing case. Additionally, Fig. 15 (corresponding to the late intake valve timing configuration) shows that the characteristic peaks previously observed in Fig. 9 are no longer present in the log data. This observation confirms that combining a later valve timing with the optimized SOI can effectively mitigate—and nearly eliminate—backfire occurrences.

Moreover, the late intake valve timing ensures inherently safer operation, characterized by minimal hydrogen residuals in the intake (as shown in Fig. 14), even during early injection. This advantage becomes particularly relevant under high-load conditions, where longer injection durations and earlier injection onset are required, as it further minimizes the likelihood of residual hydrogen accumulation and the associated backfire risks.

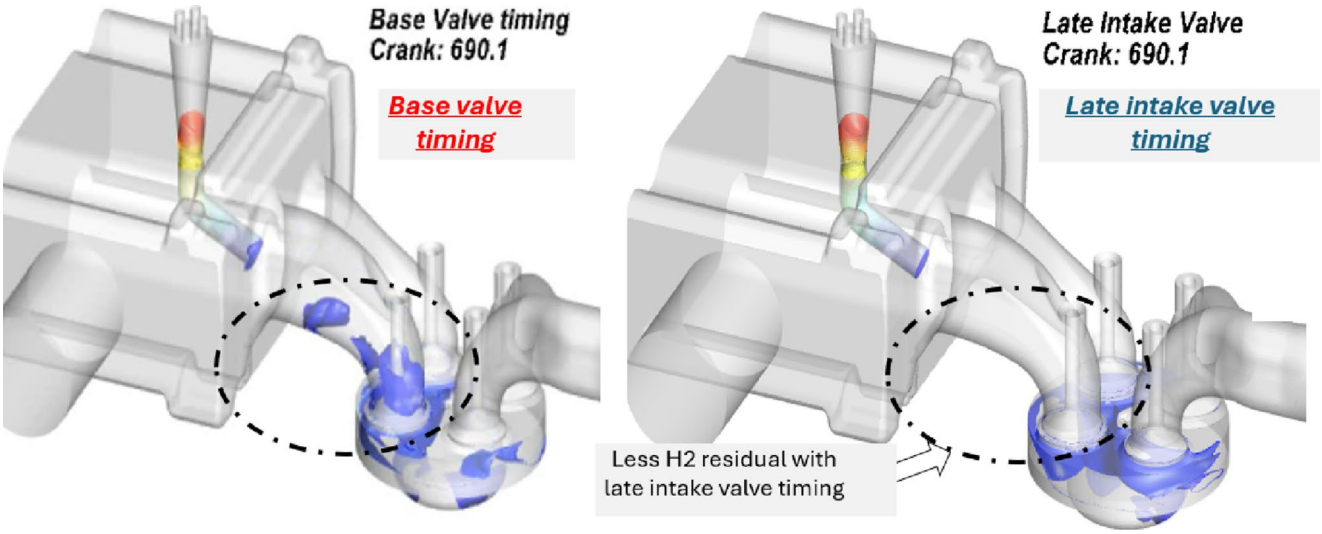

Fig. 14 Hydrogen mass fraction in iso plots for residual hydrogen mass distribution at base and late intake valve timing at optimized SOI timings

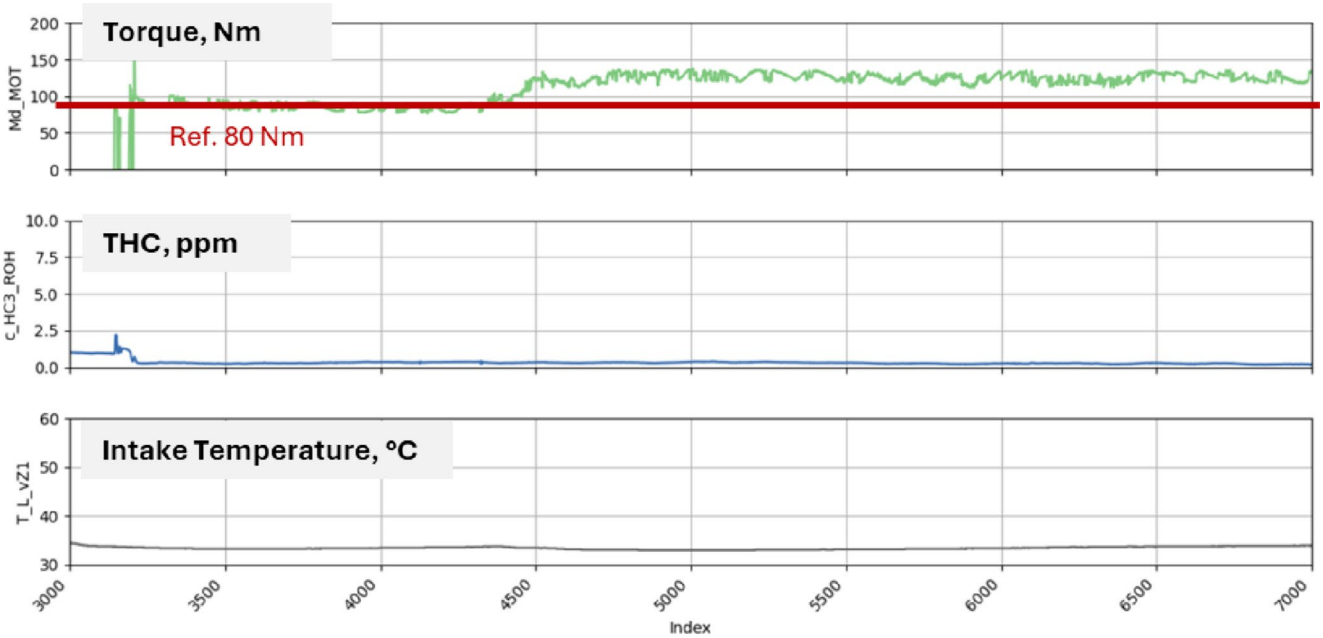

Fig. 15 Engine operation logs at the optimized late intake valve timing

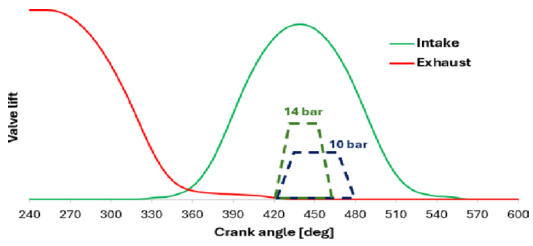

Fig. 16 Injection pressure and duration variation cases

2.5 Injection pressure and duration variation

To investigate the effects of varying injection pressure and duration on engine characteristics, two operational cases were examined, with the corresponding injection and valve timing profiles visualized in Fig. 16. Case 1 utilized a higher injection pressure of 14 bar, resulting in a correspondingly shorter injection duration of approximately 45°CA. Case 2 employed a lower injection pressure of 10 bar, which necessitated a longer duration of approximately 60°CA to deliver the identical total mass of hydrogen. Both cases

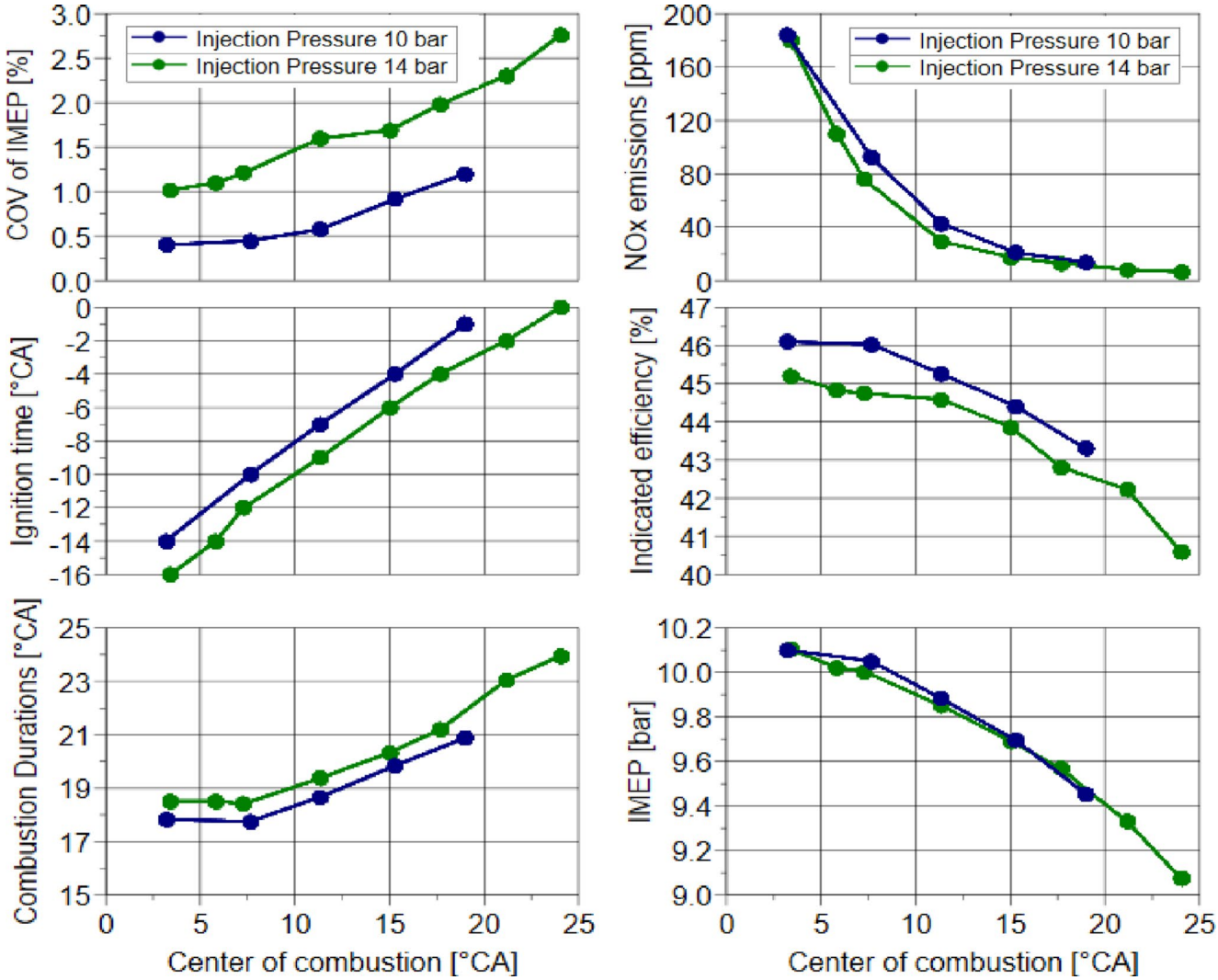

Fig. 17 Impact of injection pressure on engine performance and stability

were conducted at a constant engine load of 10 bar IMEP to ensure a direct comparison of fuel delivery effects.

The results in Fig. 17 reveal a consistent performance advantage for the lower-pressure, longer-duration injection across nearly all efficiency and stability metrics except the risk of backfire. For instance, in terms of combustion stability, represented by the Coefficient of Variation (COV) of IMEP, case 2 shows a significantly lower trend across the entire range of combustion phasing, indicating more consistent cycle-to-cycle operation. This improved stability trend directly correlates with the trend observed in indicated efficiency, which is marginally but consistently higher for case 2, particularly at advanced combustion timings. These beneficial trends are attributed to the extended mixing time provided by the longer injection duration in case 2, promoting a more homogeneous air-fuel mixture. Supporting this, the combustion duration trend for case 2 is generally shorter or comparable, reflective of a more rapid and complete burn. Furthermore, NOx emissions trend downward with retarded combustion phasing for both cases, with case 1 exhibiting a marginally lower emission trend overall. The ignition time trend shows that case 1 generally requires a more retarded ignition relative to case 2 to maintain the same combustion phasing.

However, a critical reversal of trend is observed for the risk of backfire. The risk is significantly higher for case 2 compared to case (1) This detrimental trend is due to the later End of Injection (EOI) associated with the longer duration in case (2) The reduced time window between EOI and the subsequent intake valve closure does not allow sufficient time for all of the injected hydrogen to fully enter the combustion chamber and purge the manifold, making the residual mixture more susceptible to pre-ignition. Conversely, the high-pressure, short-duration strategy of case 1 provides a larger time buffer after EOI, showing a clear trend towards effective backfire curtailment.

Consequently, the choice between these operating strategies depends on the prioritized performance metric. case 2 presents a superior outcome regarding engine efficiency (e.g., maximizing brake thermal efficiency or power output), while case 1 is empirically demonstrated to be the optimal choice for backfire suppression and overall system operational stability.

3 Conclusion

This study successfully executed a comprehensive experimental and computational fluid dynamics (CFD) analysis to investigate the fundamental mechanisms governing backfire initiation and propagation in a single-cylinder, heavy-duty hydrogen port-fuel-injection (PFI) engine. This research established a clear understanding of how mixture preparation, residual gas dynamics, and pre-ignition behavior interact. This was accomplished by systematically varying and exploring the influence of five key control parameters: injector positioning, start of injection (SOI) timing, valve phasing, back pressure, and injection pressure, on the thermo-fluidic processes within the engine. The results collectively define the operational envelope required for achieving both high-efficiency and high-stability hydrogen combustion, showing that optimal performance can be attained through coordinated parameter tuning. The main insights derived from the experimental investigation are as follows:

- *Injector placement and residuals*: In four-valve configuration engines, placing the injector near the larger intake port and directing it toward the intake valve seat minimized wall interaction, reduced residual hydrogen accumulation, and improved charge homogeneity across the cylinder. This configuration resulted in a significant reduction in backfire probability.
- *SOI timing optimization*: beginning of injection at approximately 20–30% of intake valve lift provided the best balance, ensuring good mixture uniformity while minimizing residual hydrogen entrapment. Injecting too early or too late risked backfire due to fuel pooling in the manifold or near the valve, respectively.
- *Back pressure sensitivity*: elevated back pressure increased intake temperatures by promoting internal exhaust gas recirculation (IEGR). This directly increased the engine's susceptibility to backfire.
- *Valve phasing for stability*: using a late intake valve opening proved the most effective strategy under high-load conditions, dramatically reducing backflow and backfire risk. This stability was achieved without significantly compromising mixture uniformity.
- *Cumulative effect of tuning*: coordinating the optimized SOI timing with late intake valve timing nearly eliminated backfire in both simulations and engine experiments. This validated the powerful effect of combining control strategies.
- *Injection pressure trade-off*: lower injection pressure with extended duration improved mixing but increased backfire risk as the injection event overlapped with valve closure. Higher pressure, conversely, offered a safer margin by rapidly and completely injecting hydrogen but compromised on efficiency and cycle-to-cycle stability.

In conclusion, this combined experimental and numerical framework defined the operational window essential for stable hydrogen PFI engine operation. The findings emphasize that achieving reliable and efficient hydrogen combustion is an engineering challenge that requires optimizing multiple parameters together, rather than adjusting single variables in isolation. The outcomes of this research provide actionable guidelines for current hydrogen engine calibration and establish a solid foundation for hardware development.

Acknowledgements The authors express their gratitude to the Federal Ministry for Economic Affairs and Energy for funding this work within the project PoWer following a decision of the German Bundestag. We are also indebted to the CONVERGE CFD team for granting an educational license that made this work possible. Support from the state of Baden-Württemberg through bwHPC is likewise gratefully recognized.

Author contributions B.K. prepared the experiment setup, simulation model and manuscript structure. K.K. wrote the manuscript text. F.R. provided support with experiments. U.W. and T.K. reviewed the manuscript internally.

Funding Open Access funding enabled and organized by Projekt DEAL. Open access funding provided by to the Federal Ministry for Economic Affairs and Energy.

Data availability No datasets were generated or analysed during the current study.

Declarations

Competing interests The authors declare no competing interests.

References

1. Brown, A., Ebadian, M., Saddler, J., Nylund, N.-O., Aakko-Saksa, P., Waldheim, L.: 'A report from the advanced motor fuels TCP and IEA bioenergy TCP production technologies and costs the role of renewable transport fuels (2020). in Decarbonizing Road Transport'
2. Bains, P., Bennett, S., Collina, L., Connelly, E., Delmastro, C., Evangelopoulou, S., Fajardy, M., Gouy, A., Kotani, M., Le Marois, J-B., Levi, P., Martinez Gordon, R., McDonagh, S., Pavan, F., Pizarro, A., Sloots, N., Winkler, C.: International Energy Agency, 'Global Hydrogen Review 2023', 2023.[Online]. Available: www.iea.org
3. Mughal, M.O., et al.: 'Hydrogen-Fuelled Internal Combustion Engine: a Review'. [Online]. Available: https://www.researchgate.net/publication/368848523
4. Rezaei, R., Sens, M., Riess, M., Bertram, C.: Potentials and challenges of hydrogen combustion system development as a sustainable fuel for commercial vehicles. In: Liebl, J., Beidl, C., Maus, W (eds.) Internationaler Motorenkongress 2021, Wiesbaden: Springer Fachmedien Wiesbaden, 99–114 (2021)
5. Laignel, M., Oung, R., Neveu, J.M., Vucher, A., Rieser, E., Foucher, F.: H2 efficient and near zero emissions operation on a SI PFI heavy duty single cylinder engine. Int J Hydrogen Energy **128**, 105–116 (2025). https://doi.org/10.1016/j.ijhydene.2025.04.120
6. Kubach, H., et al.: Trends und Herausforderungen bei der Entwicklung von Wasserstoffmotoren. Chemie Ingenieur Technik **96**(1–2), 167–181 (2024). https://doi.org/10.1002/cite.202300119
7. Deist, S., Zepf, A., Winkler, D., Mahler, K., Prager, M., Jaensch, M.: Endoscopic visualization of backfire behavior in a medium speed maritime hydrogen engine. Int J Hydrogen Energy (2025). https://doi.org/10.1016/j.ijhydene.2025.150938
8. Barış, O.: Prediction of NOX emissions for hydrogen combustion engines using thermodynamical model in steady and transient conditions. Int J Hydrogen Energy **110**, 138–143 (2024). https://doi.org/10.1016/j.ijhydene.2025.02.113
9. Heffel, J.W.: NOx emission reduction in a hydrogen fueled internal combustion engine at 3000 rpm using exhaust gas recirculation. Int J Hydrogen Energy **28**(11), 1285–1292 (2003). https://doi.org/10.1016/S0360-3199(02)00289-6
10. Lu, Y., Que, J., Xia, Y., Li, X., Jiang, Q., Feng, L.: A comparative study of the effects of EGR on combustion and emission characteristics of port fuel injection and late direct injection in hydrogen internal combustion engine. Applied Energy (2024). https://doi.org/10.1016/j.apenergy.2024.123830
11. Gao, J., Wang, X., Song, P., Tian, G., Ma, C.: Review of the backfire occurrences and control strategies for port hydrogen injection internal combustion engines. Fuel (2022). https://doi.org/10.1016/j.fuel.2021.121553
12. Khalid, A., et al.: Hydrogen port fuel injection: Review of fuel injection control strategies to mitigate backfire in internal combustion engine fuelled with hydrogen. Int J Hydrogen Energy **66**, 571–581 (2024). https://doi.org/10.1016/j.ijhydene.2024.04.087
13. Duan, J., Liu, F., Sun, B.: Backfire mechanism and control of PFI hydrogen internal combustion engine. Nongye Jixie Xuebao/Transactions of the Chinese Society for Agricultural Machinery **44**, 1–5 (2013). https://doi.org/10.6041/j.issn.1000-1298.2013.03.001
14. Xin, G., et al.: Monitoring of hydrogen-fueled engine backfires using dual manifold absolute pressure sensors. Int J Hydrogen Energy **47**(26), 13134–13142 (2022). https://doi.org/10.1016/j.ijhydene.2022.02.042
15. Eicheldinger, S., Karmann, S., Prager, M., Wachtmeister, G.: Optical screening investigations of backfire in a large bore medium speed hydrogen engine. International Journal of Engine Research **23**(5), 893–906 (2022). https://doi.org/10.1177/14680874211053171
16. Menaa, A., Lounici, M.S., Amrouche, F., Loubar, K., Kessal, M.: CFD analysis of hydrogen injection pressure and valve profile law effects on backfire and pre-ignition phenomena in hydrogen-diesel dual fuel engine. Int J Hydrogen Energy **44**(18), 9408–9422 (2019). https://doi.org/10.1016/j.ijhydene.2019.02.123
17. Huang, Z., et al.: Effects of hydrogen injection timing and injection pressure on mixture formation and combustion characteristics of a hydrogen direct injection engine. Fuel (2024). https://doi.org/10.1016/j.fuel.2024.130966
18. Huang, M., et al.: Experimental Investigations of the Hydrogen Injectors on the Combustion Characteristics and Performance of a Hydrogen Internal Combustion Engine. Sustainability. **16**(5), (2024). https://doi.org/10.3390/su16051940